MCB
Journals.ASM.org

Cidea Control of Lipid Storage and Secretion in Mouse and Human Sebaceous Glands

Shasha Zhang,[a] Guanghou Shui,[b] Guanqun Wang,[a] Chao Wang,[c] Shuhong Sun,[d] Christos C. Zouboulis,[e] Ran Xiao,[f] Jing Ye,[c] Wei Li,[d] Peng Li[a]

MOE Key Laboratory of Bioinformatics and Tsinghua-Peking Center for Life Sciences, School of Life Sciences, Tsinghua University, Beijing, People's Republic of China[a]; State Key Laboratory of Molecular Developmental Biology, Institute of Genetics and Developmental Biology, Chinese Academy of Sciences, Beijing, People's Republic of China[b]; Department of Pathology, Fourth Military Medical University, Xi'an, Shaanxi, People's Republic of China[c]; Department of Dermatology, Xijing Hospital, Fourth Military Medical University, Xi'an, Shaanxi, People's Republic of China[d]; Departments of Dermatology, Venereology, Allergology and Immunology, Dessau Medical Center, Dessau, Germany[e]; Research Center of Plastic Surgery Hospital, Chinese Academy of Medical Sciences & Peking Union Medical College, Beijing, People's Republic of China[f]

Sebaceous glands are skin appendages that secrete sebum onto hair follicles to lubricate the hair and maintain skin homeostasis. In this study, we demonstrated that Cidea is expressed at high levels in lipid-laden mature sebocytes and that *Cidea* deficiency led to dry hair and hair loss in aged mice. In addition, *Cidea*-deficient mice had markedly reduced levels of skin surface lipids, including triacylglycerides (TAGs) and wax diesters (WDEs), and these mice were defective in water repulsion and thermoregulation. Furthermore, we observed that *Cidea*-deficient sebocytes accumulated a large number of smaller-sized lipid droplets (LDs), whereas overexpression of Cidea in human SZ95 sebocytes resulted in increased lipid storage and the accumulation of large LDs. Importantly, Cidea was highly expressed in human sebaceous glands, and its expression levels were positively correlated with human sebum secretion. Our data revealed that Cidea is a crucial regulator of sebaceous gland lipid storage and sebum lipid secretion in mammals and humans.

The skin of most mammals is characterized by the presence of sebaceous glands, whose predominant constituent cell population is sebocytes, which produce lipid-containing sebum. Sebum is considered to be secreted from sebaceous glands by a holocrine process and contributes to the large majority of skin surface lipids, which are crucial for hair growth, moisturization of skin and hair, and the prevention of water evaporation from the skin surface (1, 2). Recent research has suggested that sebum may also contain antioxidants, antimicrobial lipids, and pheromones (2–4). The main components of sebum are triacylglycerides (TAGs), wax esters (WEs), and cholesterol esters (CEs) (2, 5, 6). Wax esters, including wax monoesters (WMEs) and wax diesters (WDEs), are skin-specific lipids secreted by sebocytes (5). In mammals, WDEs are the most abundant wax esters important for skin water repulsion (5). In humans, sebum excreted by the sebaceous glands is primarily composed of TAGs, wax esters, and squalene (Sq) (6).

In mammals, sebaceous gland volume, growth, and differentiation follow the hair cycles of the growth (anagen), regression (catagen), and resting (telogen) phases (7, 8), whereas several sebaceous-gland-specific genes, including those for stearoyl coenzyme A desaturase 1 and 3 (Scd1 and Scd3), show a hair cycle-dependent expression pattern (9). Sebaceous gland differentiation and maturation have been shown to be regulated by peroxisome proliferator-activated receptor gamma (PPARγ) (2, 10). Proteins regulating lipid synthesis, including Scd1, elongation of very-long-chain fatty acid protein 3 (ELOVL3), diacylglycerol acyltransferase 1 (Dgat 1), and fatty acid binding protein 5 (FABP5), are important regulators of sebaceous gland function and sebum secretion (11–13). Deficiencies in these genes result in sebocyte hypoplasia, decreased skin surface lipids, dry hair, and/or hair loss (14–17).

In humans, sebaceous glands from different anatomical locations have various levels of activity in sebum secretion (18). Sebaceous glands from facial skin, especially those on the nose and forehead areas, secrete a large amount of sebum, whereas sebaceous glands from the trunk and limbs secrete a smaller amount of sebum (18). Abnormal high sebum secretion in humans has been associated with several skin diseases (2, 19). In contrast, insufficient sebum secretion causes skin xerosis and xerophthalmia (20, 21).

Cell death-inducing DNA fragmentation factor (DFFA)-like effector (CIDE) family proteins, including Cidea, Cideb, and Fsp27 (Cidec), are lipid droplet (LD)-associated proteins playing important roles in LD fusion, lipid secretion, and very-low-density-lipoprotein (VLDL) maturation (22–24). Cidea is highly enriched in adult brown adipose tissue (BAT), and its deficiency results in the accumulation of smaller LDs in brown adipocytes, improved insulin sensitivity, and resistance to diet-induced obesity (25, 26). Recently, we found that Cidea is highly expressed in mammary glands during pregnancy and lactation and that it is an important regulator of LD size and milk lipid secretion (22). Here, we observed that Cidea was expressed at high levels in the sebaceous glands and that its deficiency resulted in dry hair, reduced skin surface lipid secretion, and poor water repulsion. In addition, we showed that sebocytes with *Cidea* deficiency accumulated

Received 30 December 2013 Returned for modification 20 January 2014
Accepted 10 March 2014
Published ahead of print 17 March 2014
Address correspondence to Peng Li, li-peng@mail.tsinghua.edu.cn.
Supplemental material for this article may be found at http://dx.doi.org/10.1128/MCB.01723-13.

doi:10.1128/MCB.01723-13

TABLE 1 Primer sequences used for real-time PCR

Gene product	Primer sequence	
	Forward	Reverse
Cidea	TGACATTCATGGGATTGCAGAC	GGCCAGTTGTGATGACTAAGAC
Scd3	CAGCCCCAAACGCCACAACTT	GATCTCGGGCCCATTCATACACG
CK17	ACCATCCGCCAGTTTACCTC	CTACCCAGGCCACTAGCTGA
GAPDH	TGTGTCCGTCGTGGATCTGA	CCTGCTTCACCACCTTCTTGAT
Mc5R	AGGCGCTCGGGGGTGAT	CTGCGGAGGGCGTAGATGAGAG
PPARγ	AAGCCCATCGAGGACATCCA	CGGGTGGGACTTTCCTGCTA
Scd1	CCGGAGACCCCTTAGATCGA	CCGGAGACCCCTTAGATCGA

smaller LDs and also showed that Cidea overexpression in SZ95 sebocytes increased TAG storage and LD size. More importantly, we observed that Cidea was highly expressed in human sebaceous glands and that its expression was positively correlated with sebum secretion in human skin.

MATERIALS AND METHODS

Animal breeding and maintenance. Procedures for generation of *Cidea*$^{-/-}$ and *Fsp27*$^{-/-}$ mice and routine maintenance of mouse strain were essentially the same as previously described (25, 27). Mouse experiments were carried out in the animal facility in the School of Life Sciences, Tsinghua University. Mouse-handling procedures were in accordance with the Responsible Care and Use of Laboratory Animals (RCULA) guidelines set by Tsinghua University. All research and experimental protocols involving mice were reviewed and approved by the animal research committee of Tsinghua University.

Western blot analysis. Tissues or cultured cells were lysed in radioimmunoprecipitation assay (RIPA) buffer (20 mM HEPES-KOH [pH 7.5], 150 mM NaCl, 1 mM EDTA, 10% glycerol, 0.5% sodium deoxycholate, 1% NP-40, 1% SDS, and protease inhibitor), and Western blot analysis was performed as described previously (26). Cidea and Fsp27 proteins were detected using polyclonal antibodies as previously described (27). Primary antibodies against cytokeratin 14 (CK14), CK17, and glyceraldehyde-3-phosphate dehydrogenase (GAPDH) were obtained from ZSGB-Bio, China. Antibodies against β-tubulin (Sigma), Ucp1 (Research Diagnostics Inc.), PLIN1 (Research Diagnostics Inc.), and green fluorescent protein (GFP) (Abmart, China) were also used.

Histological analysis, IHC, and IF. Skin biopsy specimens of age- and sex-matched animals were taken from similar body locations. Human skin samples were obtained as described below. Skin samples were fixed overnight at 4°C in a phosphate-buffered (pH 7.4) 4% formaldehyde solution. Sections (5 μm thick) were stained with hematoxylin and eosin (H&E). Immunohistochemistry (IHC) was performed as previously described (22). *Cidea* antibody was diluted at 1:100. Images were taken by a Nikon Eclipse 90i light microscope. IHC staining intensity was analyzed by Image Pro-Plus software. For immunofluorescence (IF), skin samples were frozen directly in OCT Tissue-Tek and 8-μm-thick sections were cut in a cryostat and postfixed in 4% paraformaldehyde (PFA) in phosphate-buffered saline (PBS). Immunofluorescent staining was performed as previously described (28). Briefly, tissue sections were first blocked in 10% goat serum for 1 h at room temperature and then incubated with Cidea antibody (diluted 1:100) overnight at 4°C. Anti-rabbit IgG antibodies conjugated with Alexa Fluor 488 (Molecular Probes) were used as secondary antibodies. Bodipy 630/650-X (Molecular Probes) (20 μg/ml) was used to visualize sebaceous gland lipids, and the nucleus was stained with 1 μM Hoechst 33342 (Molecular Probes). Fluorescent images were obtained with a Zeiss Axiovert 200M microscope.

Transmission and scanning EM. For transmission electron microscopy (EM), skin samples (1 mm^2) in the same hair cycle phase of age- and sex-matched animals were taken from similar body locations and fixed in 2.5% glutaraldehyde–0.1 M phosphate buffer (pH 7.2) for 3 h at 4°C, washed in 0.1 M phosphate buffer, postfixed in 1% osmium tetroxide in 0.1 M phosphate buffer, dehydrated through an ascending ethanol series, and embedded in an Epon epoxy mixture (15). Ultrathin sections were further stained with lead citrate and observed under a transmission electron microscope (Hitachi H-7650B) operating at 80 kV. LD diameters were measured with Image Pro-Plus software, and data are presented as previously described (29). For scanning electron microscope analyses, hairs taken from age- and sex-matched animals were attached to adhesive stubs and coated with gold. Images were taken by a scanning electron microscope (FEI Quanta 200) operating at 15 kV.

Induction of synchronized hair follicle cycling. Synchronous anagen was induced by depilation of hair shafts on the back of 7-week-old mice with all follicles in telegen as previously described (7, 30). Skin samples were taken from the depilated skin at different time points for further analysis.

Separation of epidermis and subcutaneous fat. Tail skin was cut into pieces (0.5 cm^2), washed in PBS, and incubated in 1.2 U/ml dispase II (Roche, Germany) in 1.5 mg/ml bovine serum albumin (BSA)–PBS for 1 h at 37°C or at 4°C overnight. The epidermal portions could be easily separated from the dermis with a fine forceps. The subcutaneous fat was separated by cutting from the full-thickness skin with scissors.

Genotyping, RNA extraction, and quantitative real-time PCR analyses. Genomic DNA was extracted and genotyping was performed as preciously described (25). Total RNA was extracted using TRIzol reagent (Invitrogen). The first-strand cDNAs were synthesized using a TransScript II reverse transcription (RT) kit (TransGen, China). Gene expression was assessed using real-time PCR with ABI SYBR green PCR master mix and an ABI 7500 real-time PCR system. The list of primers for real-time PCR is available in Table 1.

Skin surface lipid extraction and analysis. As previously described (14), mouse skin surface lipids were extracted by dipping each sacrificed mouse fully into 100 ml of chloroform-methanol (2:1 [vol/vol]) followed by 100 ml acetone. Human skin surface lipids were extracted from 4 people (3 males and 1 female) by using sebum-absorbing tissues of the same size 3 h after washing with soap (18, 31). Lipids on the sebum-absorbing tissues were then extracted by the use of 3 ml chloroform-methanol (2:1 [vol/vol]) followed by 3 ml of acetone. Lipid extracts were dried under nitrogen and resuspended in equal volumes of toluene. Lipid samples were dotted on the silica G plate, and the plate was run in hexane-ether-acetic acid (85:15:1 [vol/vol/vol]). The thin-layer chromatography (TLC) plates were stained with cupric sulfate (10%, wt/vol)-phosphoric acid (8% [vol/vol]) and charred at 120°C for 8 min. The density of each lipid species on TLC plates was analyzed by Quantity One software.

Analysis of skin surface lipid using mass spectrometry. Lipid extracts were diluted to appropriate volume and spiked with appropriate internal standards. Individual lipid species were quantified by referencing to spiked internal standards. High-resolution mass spectrometry (MS) was used for characterization and confirmation of lipid identities. Phospholipids and sphingolipids were analyzed using an Agilent 1260 HPLC system coupled with an Applied Biosystem 4500Qtrap triple-quadrupole/ion trap mass spectrometer as described previously (32). Briefly, separa-

tion of individual lipid classes of polar lipids was carried out using a Phenomenex Luna 3-μm-pore-size silica column (150 by 2.0 mm inner diameter [i.d.]) with the following mobile phases: phase A (chloroform-methanol-ammonium hydroxide, 89.5:10:0.5) and phase B (chloroform-methanol-ammonium hydroxide-water, 55:39:0.5:5.5). Multiple-reaction-monitoring (MRM) transitions were set up for quantitative analysis of various polar lipids. Individual lipid species were quantified by referencing to spiked internal standards. 1,2-dimyristoyl-sn-*glycero*-3-phosphocholine (PC-14:0/14:0), 1,2-dimyristoyl-sn-*glycero*-3-phosphoethanolamine (PE-14:0/14:0), 1,2-dimyristoyl-sn-*glycero*-3-phospho-L-serine (PS-14:0/14:0), 1,2-dimyristoyl-sn-*glycero*-3-phosphate (PA-17:0/17:0), 1, 2-dimyristoyl-sn-*glycero*-3-phospho-(1′-rac-glycerol) (PG-14:0/14:0), C8 glucosyl(ß) ceramide (d18:1/8:0) (C8-GluCer), C17 ceramide (d18:1/17:0) (C17-Cer), and *N*-lauroyl-D-*erythro*-sphingosylphosphorylcholine (C12-SM) were obtained from Avanti Polar Lipids (Alabaster, AL). Dioctanoyl phosphatidylinositol (PI; 16:0-PI) was obtained from Echelon Biosciences, Inc. (Salt Lake City, UT). Wax monoesters (WME) were quantified as previously described (33). Glycerol lipids TAG and diacylglyceride (DAG) were analyzed using neutral-loss-based MS/MS techniques as described previously (34, 35). Briefly, separation of lipids was carried out on a Phenomenex Kinetex 2.6-μm-pore-size C_{18} column (i.d. 4.6 by 100 mm) using an isocratic mobile phase consisting of chloroform-methanol-0.1 M ammonium acetate (100:100:4) at a flow rate of 150 μl/min for 22 min. Levels of TAG and wax diester (WDE) were calculated relative to the spiked d5-TAG 48:0 internal standard (CDN Isotopes), while DAG species were quantified using 1, 2-di-*O*-phytanyl-sn-glycerol (4ME 16:0 diether DG) as an internal standard (Avanti Polar Lipids, Alabaster, AL). Free cholesterol and cholesterol esters were analyzed as described previously with corresponding d6-cholesterol and d6-C_{18} cholesterol ester (CDN Isotopes) as internal standards (36). High-resolution mass spectrometry profile analyses of lipid extracts were also carried out using an Accela high-performance liquid chromatography (HPLC) system coupled with an LTQ Orbitrap XL hybrid Fourier transform mass spectrometer (Thermo Fisher Scientific, Waltham, MA) and both reverse-phase HPLC/MS and normal-phase HPLC/MS approaches as aforementioned. Mass spectrometry profiles were recorded with a resolution of 60,000, and mass accuracy of less than 2 ppm was obtained throughout the analytical runs.

Water retention assay. A water retention assay was performed as described previously (15, 16). Briefly, mice were immersed in water at 30°C for 2 min, and excessive water was eliminated by paper towels. Body weight and rectal temperature were recorded before and every 5 min after water immersion at room temperature. The hair water content was calculated by subtracting the body weight before water immersion from the body weight after water immersion.

Plasmid construction. Plasmid DNAs containing the Flag-tagged mouse full-length Cidea (amino acids [aa] 1 to 217) and GFP-tagged mouse full-length Cidea or its truncations (aa 118 to 217, 164 to 217, and 1 to 117) were constructed as previously described (22).

SZ95 cell culture and immunofluorescence. SZ95 sebocytes (37) were maintained in Sebomed culture medium (Biochrom, Germany) supplemented with 1 mM $CaCl_2$ or in Dulbecco's modified Eagle's medium—F-12 medium (Gibco) (1:1), both further supplemented with 10% fetal calf serum (Gibco) and 5 ng/ml human epidermal growth factor (Invitrogen), in a humidified atmosphere containing 5% CO_2 at 37°C. Subconfluent cell cultures were harvested and seeded in 6-well culture plates. GFP-tagged mouse Cidea plasmids and truncations were transfected into SZ95 cells with Lipofectamine 2000 (Invitrogen). SZ95 cells were treated with 100 μM linoleic acid (Sigma) and 1 μg/ml Bodipy 558/568 C12 (Bodipy-labeled FA) (Invitrogen) 6 h after transfection. At 24 h after transfection, cells were fixed in 4% (wt/vol) paraformaldehyde. Fluorescence images were obtained with a Zeiss Axiovert 200 microscope. LD diameters were measured with AxioVision software and are presented as previously described (29).

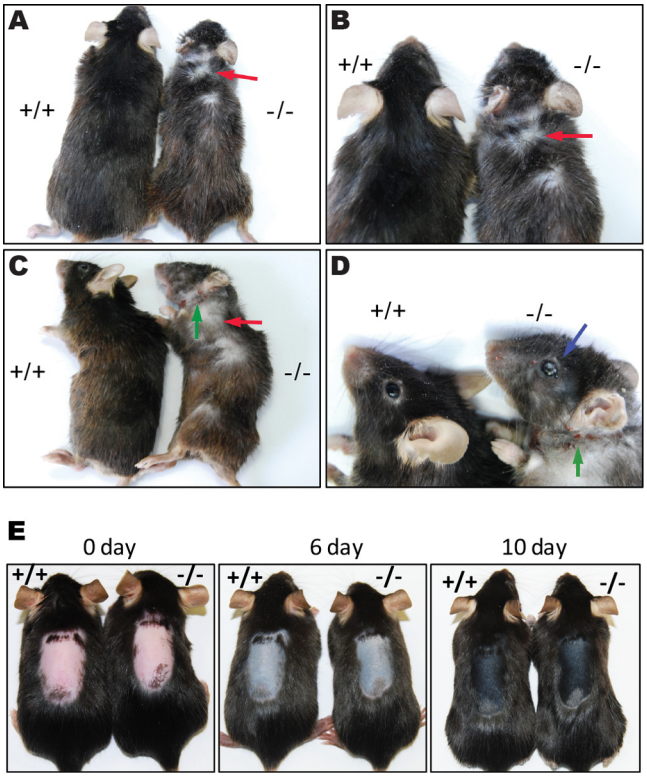

FIG 1 Old *Cidea*$^{-/-}$ mice exhibit dry hair and hair loss phenotype. (A to D) Phenotype of 10-month-old wild-type mice (+/+) and *Cidea*$^{-/-}$ (−/−) mice. *Cidea*$^{-/-}$ mice had lighter color and drier hair than wild-type mice. Hair loss (red arrow), dry eyes (blue arrow), and scratch marks (green arrow) were observed in *Cidea*$^{-/-}$ mice. (E) Mouse skin appearance at day 0 (pink, telogen), day 6 (gray, early anagen), and day 10 (black, late anagen) after induced anagen. Hairs of 7-week-old telogen mice were unplugged to induce the next anagen. Note that there is no obvious skin color difference at days 6 and 10.

TAG storage and lipolysis analyses. Subconfluent SZ95 sebocytes were harvested and seeded in a 6-cm-diameter cell culture dish. Flag-tagged mouse Cidea plasmid was transfected into SZ95 sebocytes with Lipofectamine 2000 (Invitrogen). SZ95 sebocytes were treated with 100 μM linoleic acid (Sigma) and 4 μCi/dish ^{3}H-labeled oleic acids 6 h after transfection. At 24 h after transfection, cells were washed three times with 1% BSA–PBS and fresh medium was added. Cells and medium were collected at 0 h, 2 h, and 4 h. Lipids were extracted from these samples and analyzed using TLC. TAG, WE, CE, FFA, and cholesterol dots were scraped off the plate, and the radioactive signals were detected with a MicroBeta Jet scintillometer (PerkinElmer).

Human skin specimens. Human skin specimens were collected from 23 patients at Xijing Hospital, Fourth Military Medical University (Xi'an, China). Experiments were performed in accord with the ethical requirements of the Fourth Military Medical University, and subjects gave written informed consent. Skin specimens from different body locations (4 from face skin, 4 from trunk skin, and 4 from limb skin) of 12 patients were used for Western blot analysis after cutting all the subcutaneous fat in a cryostat. Skin specimens from different body locations (4 from face skin, 4 from trunk skin, and 3 from limb skin) of 11 patients were fixed overnight at 4°C in a phosphate-buffered (pH 7.4) 4% formaldehyde solution, and immunohistochemistry (IHC) was performed with Cidea antibody.

Statistical analysis. Data are presented as means ± standard errors of the means (SEM). Statistical significance was determined using two-tailed unpaired *t* test with a significance level of 0.05.

TABLE 2 Statistical analyses of the hair phenotypes of *Cidea*$^{-/-}$ mice compared to wild-type mice[a]

Mouse group	No. of mice with hair loss/total no. of mice		% of mice with hair loss	
	+/+	−/−	+/+	−/−
Male	0/69	35/66	0	53
Female	0/52	11/41	0	27

[a] Mice 10 months of age were evaluated and statistically analyzed by their hair phenotype. −/−, *Cidea*$^{-/-}$ mice; +/+, wild-type mice.

RESULTS

Old *Cidea*$^{-/-}$ mice exhibit dry hair and hair loss phenotype. During the course of breeding *Cidea*$^{-/-}$ mice, the hair of 10-month-old or older *Cidea*$^{-/-}$ mice was unexpectedly lighter, drier, and less dense than that of wild-type mice (Fig. 1A to D). Patches of hair loss on the neck area and scratch marks on the chin were observed for both *Cidea*$^{-/-}$ male and female mice (Fig. 1B to D, red and green arrows, respectively). In addition, dry eyes were also observed in *Cidea*$^{-/-}$ mice (Fig. 1D, blue arrow). Quantitative analysis indicated that 53% and 27% of 10-month-old male and female *Cidea*$^{-/-}$ mice, respectively, showed dry hair, dry eye, and hair loss (Table 2). No obvious abnormalities in the hair and eye were observed in *Cidea*$^{-/-}$ mice younger than 10 months (data not shown). To eliminate the possibility that the dry hair and hair loss in *Cidea*$^{-/-}$ mice were due to the reduced whole-body lipid storage and lean phenotype in *Cidea*-deficient mice (25), we examined the hair phenotype in 10-month-old *Fsp27*$^{-/-}$ mice,

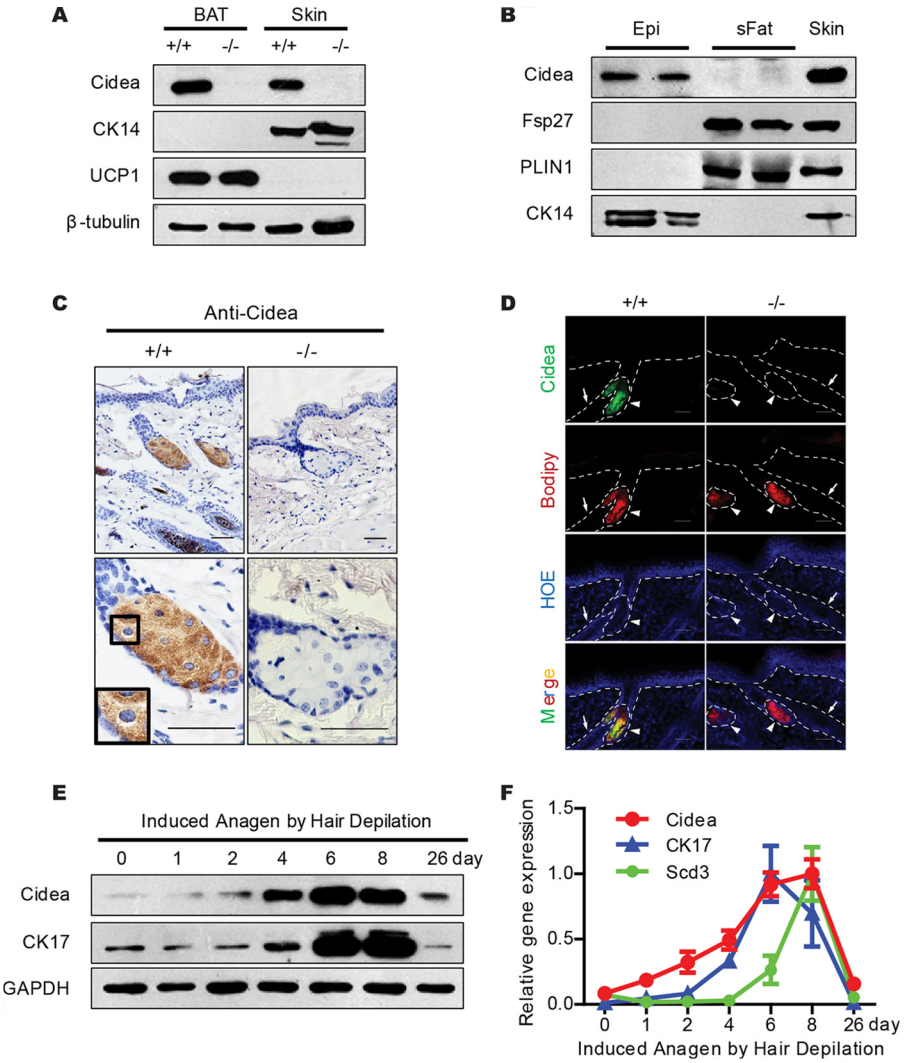

FIG 2 Sebaceous-gland-specific and hair cycle-dependent expression of Cidea. (A) Western blot analysis showing the expression of Cidea protein in full-thickness mouse skin. β-Tubulin was used as a loading control; CK14 is a marker for skin; UCP1 is a marker for BAT. (B) Western blot analysis showing expression of Cidea in mouse skin epidermis (Epi) and of Fsp27 in subcutaneous fat (sFat). Epidermis was separated by incubating tail skin in 1.2 U/ml dispase. PLIN1 is a marker for subcutaneous white fat; CK14 is a marker for epidermis. (C) Immunohistochemical (IHC) staining of paraffin sections of skin from wild-type (+/+) and *Cidea*$^{-/-}$ (−/−) mice with Cidea antibody. Scale bar, 50 μm. (D) Immunofluorecence (IF) staining of frozen skin sections from wild-type and *Cidea*$^{-/-}$ mice using Cidea antibody. Neutral lipids were stained with Bodipy, and the nucleus was stained with Hoechst (HOE). Hair follicles are indicated by arrows and sebaceous glands by arrowheads. Scale bar, 50 μm. (E and F) Levels of Cidea protein (E) and mRNA (F) during induced anagen by hair depilation. GAPDH was used as a loading control; Scd3 and CK17 are markers for hair cycles. $n = 5$ for each indicated time point in panel F. Bars show means ± SEM.

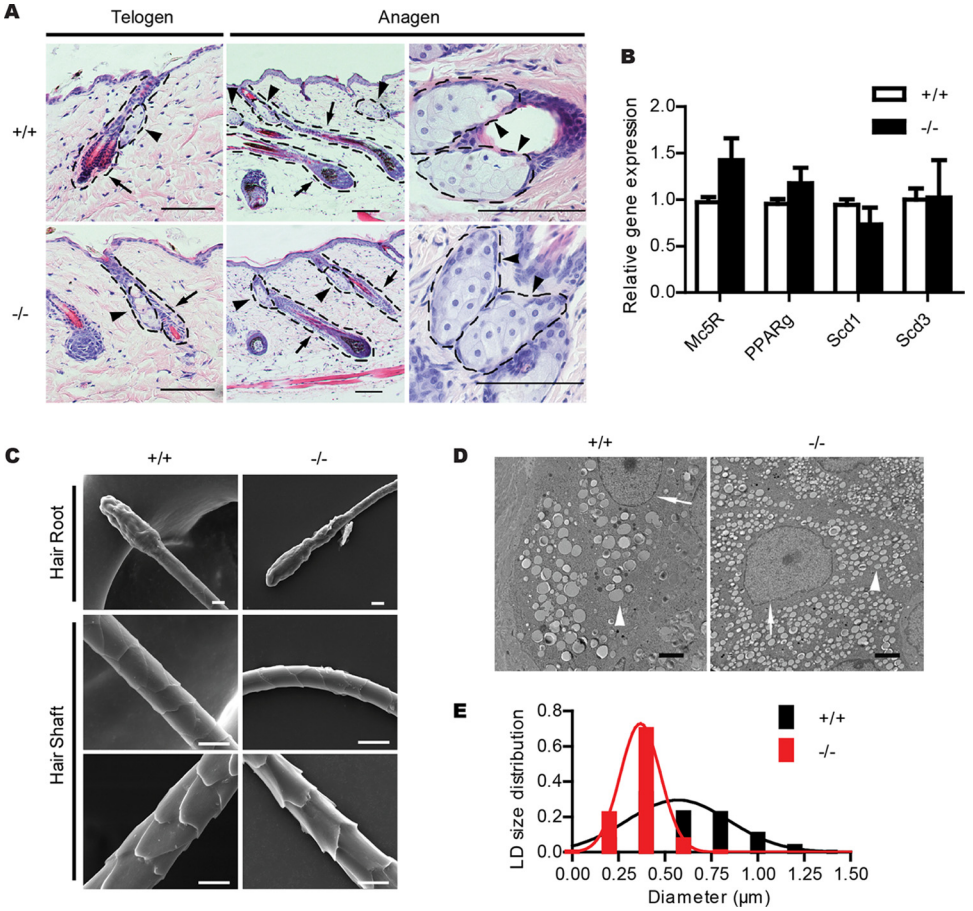

FIG 3 Accumulation of smaller LDs in the sebaceous gland of *Cidea*$^{-/-}$ mice. (A) H&E staining of telogen and anagen skin sections from wild-type (+/+) and *Cidea*$^{-/-}$ (−/−) mice. Hair follicles are indicated by arrows and sebaceous glands by arrowheads. Scale bar, 100 μm. (B) Relative mRNA levels of sebaceous-gland-specific proteins (Mc5R, PPARγ, Scd1, and Scd3); $n = 4$ for each genotype. Bars represent means ± SEM. (C) Scanning electron microscopic images of hairs from wild-type mice (+/+) and *Cidea*$^{-/-}$ mice (−/−). No obvious differences can be seen in hair roots and hair shafts. Scale bar, 10 μm. (D) Electron microscopic (EM) images of skin sections from wild-type (+/+) and *Cidea*$^{-/-}$ (−/−) mice. Nuclei are indicated by arrows, and LDs are indicated by arrowheads. Scale bar, 2 μm. (E) Lipid droplet (LD) size distribution. $n = 4$ for each genotype. Diameters of over 570 LDs for each genotype were measured.

which also have a strong lean phenotype (27), and found that 10-month-old or older *Fsp27*$^{-/-}$ mice did not show dry hair, dry eyes, or hair loss (see Fig. S1 in the supplemental material). Therefore, dry hair and hair loss were not the result of the lean phenotype and were specific to *Cidea*$^{-/-}$ mice. As a disturbed hair growth cycle may cause hair loss (28), we unplugged the hair of 7-week-old mice in the telogen phase of the hair cycle to induce anagen. We did not observe a difference in skin color and hair growth between wild-type mice and *Cidea*$^{-/-}$ mice (Fig. 1E). Overall, these data suggest that Cidea is an important regulator of hair and skin quality.

Sebaceous-gland-specific and hair cycle-dependent expression of Cidea. The dry hair and hair loss observed in *Cidea*$^{-/-}$ mice led us to speculate that Cidea may be specifically expressed in the skin. Indeed, Cidea proteins were detected in the skin of wild-type mice and were coexpressed with the skin-specific cytokeratin 14 (CK14) protein (Fig. 2A). We then separated the skin epidermis from the subcutaneous fat with dispase and observed that Cidea proteins were specifically detected in the epidermis and that Fsp27 was detected in subcutaneous white fat (Fig. 2B).

Immunohistochemistry analysis using a Cidea antibody showed a strong Cidea-positive signal in the center of the sebaceous glands, located on the LDs of mature sebocytes in the sebaceous gland which are highly differentiated and contain many large LDs (Fig. 2C). Immunofluorescent staining also confirmed the presence of Cidea proteins in the sebaceous glands, and the Cidea proteins colocalized with the Bodipy-stained LDs in the sebaceous glands (Fig. 2D). We further examined Cidea expression during hair cycle induction and found that the sebaceous glands showed a substantial hair cycle-dependent functional fluctuation (1). We observed that Cidea mRNA and protein levels increased during the course of an induced hair cycle, reaching the highest level at the anagen phase (days 6 to 8 after anagen induction) followed by a decrease in the catagen and telogen phases (Fig. 2E and F). This temporal expression of Cidea was highly correlated with that of cytokeratin 17 (CK17) and Scd3, which have been previously shown to have hair cycle-dependent expression (9, 38). Overall, these data indicate that Cidea is expressed specifically and at high levels in the sebaceous gland with a hair cycle-dependent expression pattern.

Accumulation of smaller LDs in the sebaceous gland of *Cidea*$^{-/-}$ mice. Next, we examined the morphology of the skin epidermis and sebaceous glands of 3-month-old wild-type and *Cidea*$^{-/-}$ mice by H&E staining. The morphology characteristics

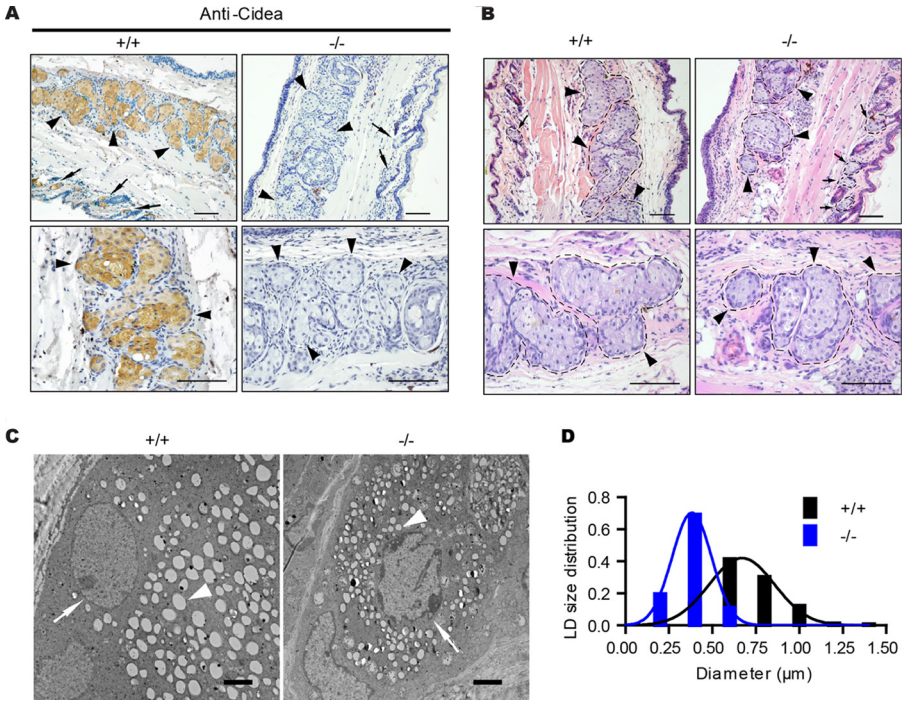

FIG 4 Meibomian-gland-specific expression of Cidea and reduced LD size in the meibomian gland of *Cidea*$^{-/-}$ mice. (A) Immunohistochemical (IHC) staining of paraffin sections of eyelid from wild-type (+/+) and *Cidea*$^{-/-}$ (−/−) mice with Cidea antibody. Scale bar, 100 μm. Meibomian glands are indicated by arrowheads, and sebaceous glands are indicated by arrows. (B) H&E staining of eyelid sections from wild-type (+/+) and *Cidea*$^{-/-}$ (−/−) mice. Meibomian glands are indicated by arrowheads, and sebaceous glands are indicated by arrows. Scale bar, 100 μm. (C) Electron microscopic (EM) images of eyelid sections from wild-type (+/+) and *Cidea*$^{-/-}$ (−/−) mice. Nuclei are indicated by arrows, and LDs are indicated by arrowheads. Scale bar, 2 μm. (D) Lipid droplet (LD) size distribution. $n = 3$ for each genotype. Diameters of over 800 LDs for each genotype were measured.

of the epidermis, hair follicle, and sebaceous glands appeared to be similar between *Cidea*$^{-/-}$ and wild-type mice (Fig. 3A). Expression levels of PPARγ, a crucial regulator of sebaceous gland differentiation, and expression levels of highly expressed sebaceous gland genes for Scd1, Scd3, and melanocortin-5 receptor (Mc5R) (39) were similar between *Cidea*$^{-/-}$ and wild-type mice (Fig. 3B). The morphology characteristics of hair revealed by scanning electron microscopy were also similar in wild-type and *Cidea*$^{-/-}$ mice (Fig. 3C). These data suggest that *Cidea* deficiency did not affect sebaceous gland differentiation and hair morphology. However, the higher-resolution analysis in sebaceous glands by electron microscopy (EM) analysis revealed that *Cidea*$^{-/-}$ sebocytes accumulated a larger number of smaller-size LDs than those of wild-type mice (Fig. 3D). Quantitative analysis of the LD size distribution (29) in sebocyte LDs demonstrated that the diameter of the largest LD in *Cidea*$^{-/-}$ sebocytes was 0.86 μm and that the diameter of the largest LD in wild-type sebocytes was 2.1 μm (Fig. 3E), thereby suggesting that Cidea controls LD growth and lipid storage in sebocytes.

Meibomian-gland-specific expression of Cidea and reduced LD size in the meibomian gland of *Cidea*$^{-/-}$ mice. Meibomian glands are greatly enlarged sebaceous glands in the eyelid, producing lipids that constitute the outer layer of the preocular tear film (40). And dysfunction of meibomian glands often leads to dry eyes (41). As we observed the dry eye phenotype in old *Cidea*$^{-/-}$ mice, we checked the Cidea expression in meibomian glands by immunohistochemistry analysis using a Cidea antibody. Consistent with its expression in sebaceous gland, Cidea-positive signals were indeed detected in the meibomian glands (Fig. 4A). The positive Cidea signal was not detected in the meibomian glands of *Cidea*$^{-/-}$ mice (Fig. 4A). The gross morphology characteristics of meibomian glands as shown by H&E staining in wild-type and *Cidea*$^{-/-}$ mice were similar (Fig. 4B). However, higher-resolution EM analysis in meibomian glands showed that *Cidea*$^{-/-}$ meibocytes accumulated a larger number of smaller-size LDs than those of wild-type mice (Fig. 4C and D), in similarity to the results observed in *Cidea*$^{-/-}$ sebocytes.

Reduced skin surface lipids in *Cidea*$^{-/-}$ mice. Next, we examined sebum secretion by measuring the amount and composition of skin surface lipids of wild-type and *Cidea*$^{-/-}$ mice by thin-layer chromatography (TLC). The TAG levels in the skin surface lipids were significantly reduced in *Cidea*$^{-/-}$ mice compared with wild-type mice (83% reduction) (Fig. 5A and B). The level of WDE, a major wax ester in mouse sebum, was also significantly reduced in the skin surface lipids of *Cidea*$^{-/-}$ mice (30% reduction compared with that in wild-type mice) (Fig. 5A and B). Levels of skin FFAs, CEs, and free cholesterol were similar between wild-type and *Cidea*$^{-/-}$ mice (Fig. 5A). Interestingly, we observed a further reduction of skin WDE levels in 10-month-old *Cidea*$^{-/-}$ mice (61% lower than that of wild-type mice) (Fig. 5A and B). A reduction of levels of skin TAGs and WDEs was also observed in *Cidea*$^{-/-}$ female mice (Fig. 5C and D).

A detailed skin lipid profile was further determined by high-resolution lipidomic analyses. Consistent with the TLC results, levels of TAGs, diacylglycerides (DAGs), and WDEs were dramatically decreased in the skin of *Cidea*$^{-/-}$ mice compared with those seen in wild-type mice (see Fig. S2A in the supplemental material). The amounts of skin wax monoesters (WMEs) were similar be-

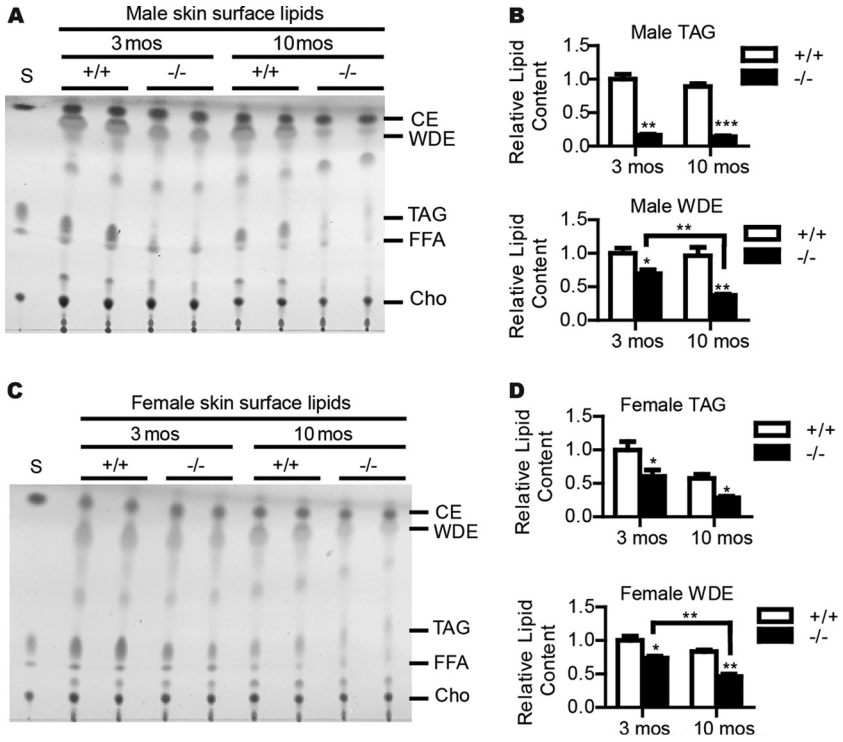

FIG 5 Reduced skin surface lipids in *Cidea*$^{-/-}$ mice. (A and C) Thin-layer chromatography (TLC) analysis of skin surface lipids from both 3-month-old and 10-month-old wild-type (+/+) and *Cidea*$^{-/-}$ (−/−) male (A) and female (C) mice. S, lipid standards. CE, cholesterol esters. WDE, wax diesters. TAG, triglyceride. FFA, free fatty acid. Cho, cholesterol. (B and D) Quantifications of male (B) and female (D) mice. $n = 5$ for each male genotype. $n = 4$ for each female genotype. Bars represent means ± SEM. *, $P < 0.05$; **, $P < 0.001$; ***, $P < 0.0001$.

tween wild-type and *Cidea*$^{-/-}$ mice (see Fig. S2A). Liquid chromatography-mass spectrometry analysis further showed that the concentrations of all individual TAG (see Fig. S2B) or most individual DAG (see Fig. S2E) species were markedly lower in the skin of *Cidea*$^{-/-}$ mice. A significant decrease in the levels of longer-chain WDEs and a slight increase in the levels of a small portion of shorter-chain WDEs was observed in the skin of *Cidea*$^{-/-}$ mice (see Fig. S2D). The amount of phosphatidylserine (PS) (see Fig. S2A and F), one of the major components of the plasma membrane, was also substantially lower in the skin surface lipids of *Cidea*$^{-/-}$ mice. In addition, levels of phosphatidylcholine (PC) and phosphatidyl glycerol (PG) (see Fig. S2A) were slightly lower, whereas the concentrations of other phospholipids, such as lysophosphatidylcholine (LPC), phosphatidylethanolamine (PE), phosphatidylinositol (PI), sphingomyelin (SM), ceramide (Cer), and phosphatidic acid (PA), were similar in the skin surface lipids of *Cidea*$^{-/-}$ mice and wild-type mice (see Fig. S2A). Overall, these data indicate that Cidea plays an important role in controlling lipid storage and secretion, especially that of TAG and WDE, onto the hair and skin surface.

Defective water repulsion and thermoregulation in *Cidea*$^{-/-}$ mice. To examine if reduced skin surface lipid levels affected water retention in *Cidea*$^{-/-}$ mice, we performed a water repulsion experiment in which the animals were immersed into 30°C water for 2 min and body weight was measured before and every 5 min after water immersion (15). *Cidea*$^{-/-}$ male mice were still wet 25 min after water immersion, but the wild-type mice were nearly dry (Fig. 6A). *Cidea*$^{-/-}$ male mice absorbed 8% of water relative to their body weight, and wild-type mice absorbed only 4% of water relative to their body weight, which equated to 2-fold-higher water retention for the *Cidea*$^{-/-}$ mice (Fig. 6B). *Cidea*$^{-/-}$ female mice also showed lower water repulsion (Fig. 6D).

As defective sebum secretion may result in impaired thermoregulation after water immersion (15, 16, 39), we measured the core body temperature before and every 5 min after the animals were immersed in water for 2 min. The core body temperatures for wild-type and *Cidea*$^{-/-}$ mice were similar before the mice were immersed in water. After water immersion, the core body temperature of wild-type male mice dropped to 30°C and returned to normal approximately 25 min after water exposure (Fig. 6C), coinciding with the hair-drying duration. In contrast, the core temperature of *Cidea*$^{-/-}$ mice decreased to 28.4°C after immersion and remained low (Fig. 6C). Forty minutes was required for these animals to recover to normal body temperature (Fig. 6C), correlating with the hair-drying duration. *Cidea*$^{-/-}$ female mice also showed lower body temperature after immersion in water and a slower recovery (Fig. 6E). These data suggest that animals with *Cidea* deficiency are defective in water repulsion and thermoregulation after water immersion, which is consistent with their lower levels of skin surface lipids and reduced lipid storage in the sebaceous glands.

Cidea promotes lipid storage in SZ95 sebocytes. To further confirm the role of Cidea in promoting lipid storage in sebocytes, we overexpressed Cidea in the human SZ95 sebocytes (37) and measured the total cellular amount of TAGs and the rate of lipolysis. The amount of TAGs in SZ95 sebocytes expressing Cidea was approximately 2-fold higher than that of control cells (Fig. 7A). In

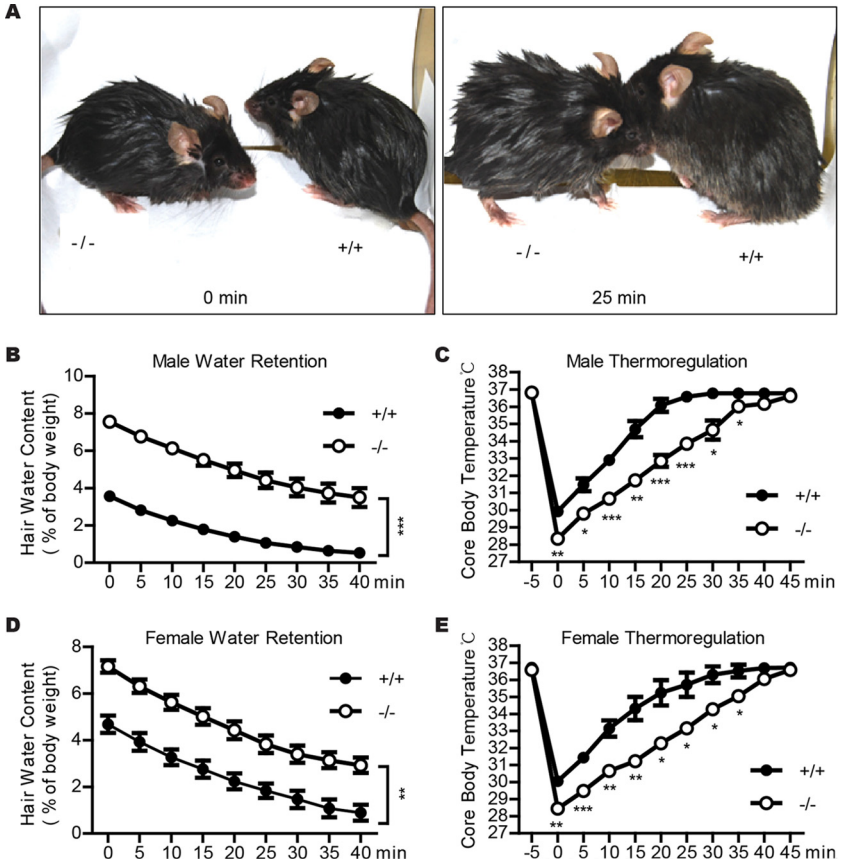

FIG 6 Defective water repulsion and thermoregulation in *Cidea*$^{-/-}$ mice. (A) Images of animals immediately after (left, 0 min) or 25 min after (right) a 2-min immersion in 30°C water. (B and D) Impaired water repulsion in *Cidea*$^{-/-}$ mice (−/−). After water immersion, body weight was measured every 5 min for 40 min. Male (B) and female (D) *Cidea*$^{-/-}$ mice (−/−) absorb twice as much water as wild-type mice (+/+) after water immersion. Bars represent means ± SEM. For male mice, $n = 7$ for each genotype; for female mice, $n = 4$ for each genotype. **, $P < 0.01$; ***, $P < 0.001$. (C and E) Defective thermoregulation of *Cidea*$^{-/-}$ mice (−/−) after water immersion. After water immersion, rectal temperature was measured every 5 min for 45 min. The data shown at −5 min represent the body temperature just before water immersion. $n = 4$ for each genotype of both male and female mice. Bars represent means ± SEM. *, $P < 0.05$; **, $P < 0.01$; ***, $P < 0.001$.

contrast, the rate of lipolysis in SZ95 sebocytes expressing Cidea was 55% lower than that of control cells (Fig. 7A). We next evaluated the LD size in SZ95 sebocytes expressing Cidea and observed that overexpression of full-length Cidea (aa 1 to 217) in SZ95 sebocytes dramatically increased LD sizes (Fig. 7B to D). When truncated Cidea proteins containing the C-terminal region of Cidea (either aa 118 to 217 or 164 to 217) were expressed in SZ95 cells, they were localized to LDs and showed low activity in promoting LD growth (Fig. 7C and D). However, the N-terminal domain of the Cidea protein (aa 1 to 117) did not localize to LDs and had no activity in promoting LD growth (Fig. 7C and D). Thus, the C-terminal domain of Cidea is important for its LD localization and LD growth. These data suggest that Cidea plays a positive role in promoting lipid storage and LD growth in sebocytes and that full-length protein is required for its high activity.

Expression of Cidea in human sebaceous glands and its positive correlation to sebum secretion. Abnormal sebum secretion in human skin has been associated with several skin diseases, with the most prominent among them being acne (2, 20, 21). To evaluate the physiological role of Cidea in human sebum secretion, we first examined the expression of Cidea in skin samples collected from different anatomic locations by Western blot analysis using a Cidea antibody. A strong Cidea-positive band was observed in nose and cheek skin (face skin) (Fig. 8A and B). A relatively weaker Cidea band was detected in back and chest skin (trunk skin), and a significantly lower intensity of the Cidea band was detected in arm and leg skin (limb skin) (Fig. 8A and B). Immunohistochemical analysis further confirmed that Cidea protein was present at the highest levels in the face (nose and cheek) sebaceous glands, at moderate levels in the trunk (chest and back) sebaceous glands, and at low levels in the limb (arm and leg) area (Fig. 8C and D). These data clearly demonstrate that Cidea is expressed in the mature sebocytes of human sebaceous glands, with the highest expression in that of face sebaceous glands, which are the ones with the highest grade of differentiation and thus with the largest number of mature sebocytes and the highest sebum secretion rates.

Next, we extracted skin surface lipids from different parts of human skin using sebum-absorbing tissues of the same size (18, 31) and characterized these lipids by TLC analysis. Human skin surface lipids also contain TAGs, WEs, CEs, FFAs, and cholesterol In comparison to mouse skin surface lipids, human skin surface lipids contain much lower levels of WDE species and abundant Sq (5, 42). We observed high levels of all lipid species extracted from face skin (nose and cheek), lower levels (approximately 45% to 65% reduction) from trunk skin (back and chest), and much lower levels (approximately 66% to 93% reduction) from limb

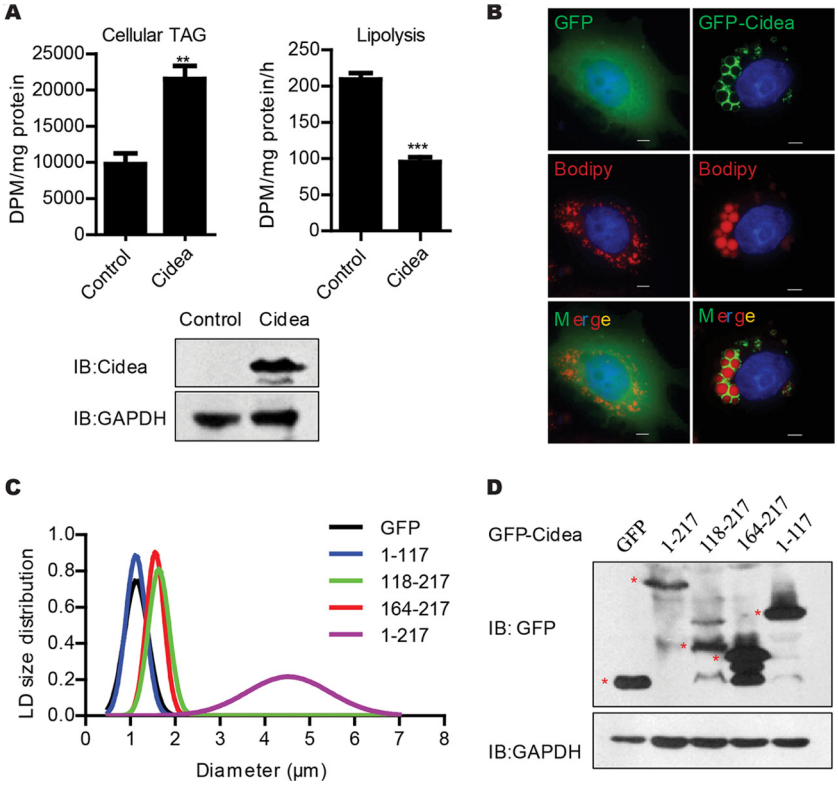

FIG 7 Cidea promotes lipid storage in SZ95 sebocytes. (A) Increased cellular TAG storage and decreased lipolysis in SZ95 sebocytes expressing Flag-tagged Cidea in the presence of 100 μM linoleic acid and 4 μCi/dish ^{3}H-labeled oleic acid. $n = 4$ for each analysis. Bars represent means ± SEM. **, $P < 0.01$; ***, $P < 0.001$. Western blot analysis (bottom panel) showed the expression levels of Cidea. GAPDH was used as the loading control. DPM, disintigrations per minute; IB, immunoblot. (B) Increased LD size in SZ95 sebocytes expressing GFP-Cidea in the presence of 100 μM linoleic acid and Bodipy 558/568 C12 (Bodipy-labeled FA). Scale bar, 10 μm. (C and D) LD size distribution in SZ95 sebocytes expressing GFP-tagged full-length (aa 1 to 217) Cidea and Cidea truncations. LD diameters of over 50 cells were measured for full-length Cidea and its truncations. (D) Western blot analysis with GFP antibody showed expression of full-length Cidea and its truncations. Red stars indicate the correctly sized proteins. GAPDH was used as the loading control.

skin (arm and leg) (Fig. 8E and F), which was similar to previously described results (18). These data indicate that the expression levels of human Cidea in sebaceous glands are positively correlated with the amount of skin surface lipids and sebum secretion.

DISCUSSION

Sebaceous lipids secreted by sebaceous glands contribute to the integrity of the skin barrier, including lubrication, water repulsion capability, and antimicrobial activity (1, 2, 4). Here, we observed that Cidea was expressed at high levels in mature sebocytes with a hair cycle-dependent expression pattern. *Cidea*$^{-/-}$ mice developed dry hair, hair loss, dry eye, and skin lesions at an old age, and these mice had reduced sebum lipid secretion. In addition, we observed that *Cidea*-deficient sebocytes accumulated smaller LDs and also observed that overexpression of Cidea in human SZ95 sebocytes resulted in higher levels of TAG storage and increased LD size. In addition, we detected specific and high expression of Cidea in human sebaceous glands which positively correlated with the secretion of sebum lipids.

Specific and higher expression of Cidea in sebaceous glands was confirmed by immunohistochemistry, immunofluorescent staining, and Western blot analyses. Cidea expression was also observed in meibomian glands, which are greatly enlarged sebaceous glands in the eyelid and produce lipids that constitute the outer layer of the preocular tear film. In addition, Cidea expression was dependent of the hair cycles, with the highest expression at the anagen phase, which was similar to results determined for another sebaceous-gland-specific gene, *Scd3* (9). The specific and high expression of Cidea in sebaceous glands is consistent with its high expression levels in mammary glands during pregnancy and lactation, as both are derived from the ectoderm (43). Nipple epithelium has also been shown to be converted into pilosebaceous units (43). In contrast, other CIDE family proteins, including Fsp27 and Cideb, are not detected in mammary-gland epithelial cells and sebaceous glands. Common regulatory factors, including transcriptional factors (PPARα and PPARγ) and cofactors (RIP140 and PGC1-α), may be responsible for the specific expression of Cidea in these ectoderm-derived and lipid-secreting tissues (44, 45).

It is interesting that the dry hair, hair loss, dry eye, and skin lesion phenotypes were observed in old *Cidea*$^{-/-}$ mice (10 months of age or older), whereas mice younger than 10 months did not exhibit these defects. Intriguingly, reduced skin surface lipid levels were observed in both young (3-month-old) and old (10-month-old) *Cidea*$^{-/-}$ mice. Dry hair and hair loss are usually observed in old animals or humans, which may be due to the active and high levels of sebum secretion in young adults. Indeed, we observed higher levels of sebum lipids in 3-month-old mice than in 10-month-old mice. In addition, the WDE levels were reduced more drastically in 10-month-old *Cidea*$^{-/-}$ mice, which

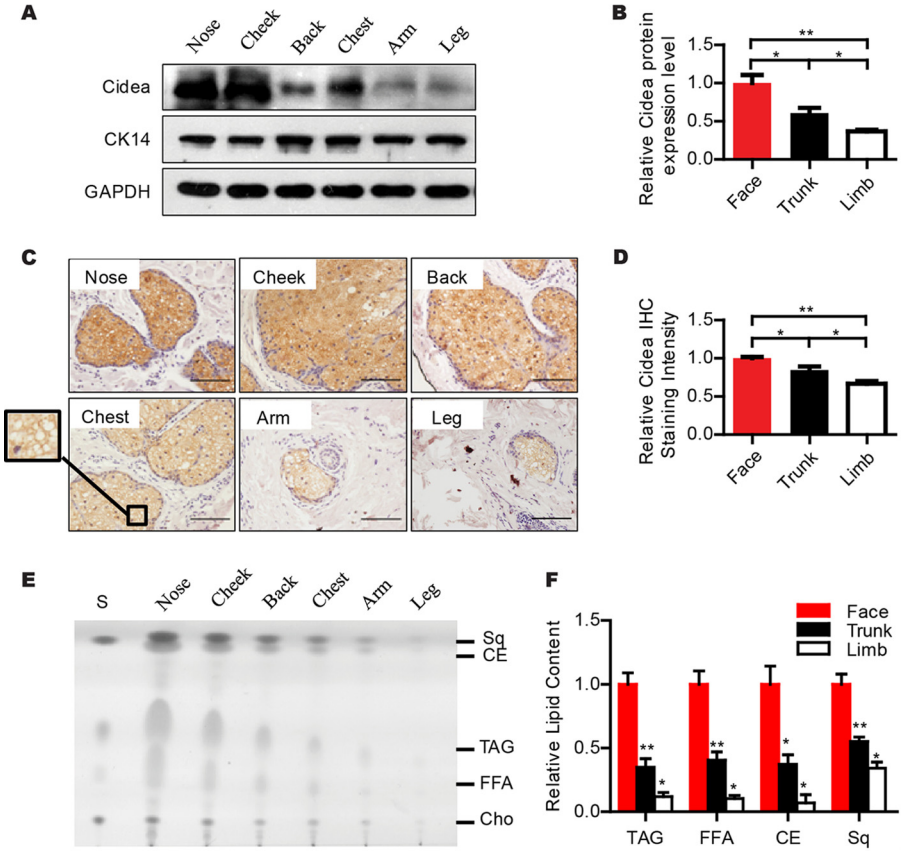

FIG 8 Expression of Cidea in human sebaceous glands and its positive correlation with sebum secretion. (A and B) Western blot analysis with Cidea antibody showing different expression levels of Cidea in the human skin of different anatomical locations. CK14 is the marker for skin, and GADH is the loading control. Quantifications are shown in panel B. $n = 4$ for each anatomical location. Bars represent means ± SEM.*, $P < 0.05$; **, $P < 0.01$. (C and D) Immunohistochemistry (IHC) staining of human skin sections of different anatomical locations using Cidea antibody. Scale bar, 100 μm. Quantitative analysis for immunostaining intensity of human Cidea is shown in panel D. $n = 4$ for both face (nose and cheek) and trunk (chest and back) skin; $n = 3$ for limb (arm and leg) skin. Bars represent means ± SEM. *, $P < 0.05$; **, $P < 0.01$. (E and F) Thin-layer chromatography (TLC) analysis of human skin surface lipids from different body parts. S, lipid standards. Sq, squalene. CE, cholesterol ester. TAG, triglyceride. FFA, free fatty acid. Cho, cholesterol. Quantifications are shown in panel F; $n = 4$ for each body part. Bars represent means ± SEM. *, $P < 0.05$; **, $P < 0.01$; ***, $P < 0.001$.

may have potentially contributed to the hair loss and dry skin phenotype of *Cidea*$^{-/-}$ mice. We also observed a higher occurrence of dry hair and hair loss phenotypes in male mice than in female mice, thereby suggesting a combined effect of sex hormones and sebum secretion in controlling hair loss.

The dry hair and hair loss phenotypes in *Cidea*$^{-/-}$ mice are likely due to the reduced levels of skin surface lipids and lower sebum secretion, and our quantitative lipidomic analyses demonstrated a significant and overall reduction of levels of skin and hair lipids, including all individual species of TAG and most individual species of WDEs. Reduced skin lipid levels in *Cidea*$^{-/-}$ mice also contributed to their reduced ability for water repulsion and thermoregulation. The dry eye phenotype in *Cidea*$^{-/-}$ mice is likely contributed by its role in controlling lipid storage in the meibomian glands. We have previously shown that CIDE family proteins are crucial regulators of LD fusion and growth in adipocytes (24). Here, we observed that mature sebocytes of *Cidea*$^{-/-}$ mice accumulated smaller LDs. In contrast, overexpression of Cidea in sebocytes increased lipid storage and promoted LD growth. Therefore, Cidea likely controls LD fusion and growth in sebocytes, and loss of Cidea results in the accumulation of smaller LDs and reduced sebum secretion.

In human skin, higher levels of sebum secretion are linked to the formation of acne, which affects adolescence and is more severe in males (2, 19). We have established a clear positive correlation of Cidea expression and sebum secretion, as Cidea proteins were detected in human sebaceous glands, with the highest expression in the face skin, which secretes the largest amount of sebum. In contrast, low levels of Cidea expression were observed in the limb sebaceous glands. Interestingly, human sebocytes *in vitro* respond to androgens in a manner dependent on the body localization of their paternal sebaceous glands (46). These data strongly indicate that Cidea plays a crucial role in human sebum secretion and the maintenance of skin homeostasis. It will be interesting to test if defective human Cidea contributes to the development of skin xerosis and xerophthalmia, which are primarily due to decreased sebum secretion, and if there are gender differences. Cidea may serve as a novel therapeutic target for the screening of drugs to combat sebaceous gland diseases, such as acne.

ACKNOWLEDGMENTS

We thank members of Peng Li's laboratory at Tsinghua University for helpful discussion.

This work was supported by grants from the National Basic Research

Program (2013CB530602 to P.L and 2011CB910801 to P.L.) and from the National Natural Science Foundation of China (31030038).

REFERENCES

1. **Schneider MR, Paus R.** 2010. Sebocytes, multifaceted epithelial cells: lipid production and holocrine secretion. Int. J. Biochem. Cell Biol. **42:**181–185. http://dx.doi.org/10.1016/j.biocel.2009.11.017.
2. **Smith KR, Thiboutot DM.** 2008. Thematic review series: skin lipids. Sebaceous gland lipids: friend or foe? J. Lipid Res. **49:**271–281. http://dx.doi.org/10.1194/jlr.R700015-JLR200.
3. **Feingold KR.** 2009. The outer frontier: the importance of lipid metabolism in the skin. J. Lipid Res. **50:**S417–S422. http://dx.doi.org/10.1194/jlr.R800039-JLR200.
4. **Drake DR, Brogden KA, Dawson DV, Wertz PW.** 2008. Thematic review series: skin lipids. Antimicrobial lipids at the skin surface. J. Lipid Res. **49:**4–11. http://dx.doi.org/10.1194/jlr.R700016-JLR200.
5. **Thody AJ, Shuster S.** 1989. Control and function of sebaceous glands. Physiol. Rev. **69:**383–416.
6. **Picardo M, Ottaviani M, Camera E, Mastrofrancesco A.** 2009. Sebaceous gland lipids. Dermatoendocrinol. **1:**68–71. http://dx.doi.org/10.4161/derm.1.2.8472.
7. **Müller-Röver S, Handjiski B, van der Veen C, Eichmüller S, Foitzik K, McKay IA, Stenn KS, Paus R.** 2001. A comprehensive guide for the accurate classification of murine hair follicles in distinct hair cycle stages. J. Invest. Dermatol. **117:**3–15. http://dx.doi.org/10.1046/j.0022-202x.2001.01377.x.
8. **Plikus MV, Chuong C-M.** 2008. Complex hair cycle domain patterns and regenerative hair waves in living rodents. J. Invest. Dermatol. **128:**1071–1080. http://dx.doi.org/10.1038/sj.jid.5701180.
9. **Zheng Y, Prouty SM, Harmon A, Sundberg JP, Stenn KS, Parimoo S.** 2001. Scd3—a novel gene of the stearoyl-CoA desaturase family with restricted expression in skin. Genomics **71:**182–191. http://dx.doi.org/10.1006/geno.2000.6429.
10. **Dozsa A, Dezso B, Toth BI, Bacsi A, Poliska S, Camera E, Picardo M, Zouboulis CC, Biro T, Schmitz G, Liebisch G, Ruhl R, Remenyik E, Nagy L.** 15 October 2013. PPARgamma-mediated and arachidonic acid-dependent signaling is involved in differentiation and lipid production of human sebocytes. J. Invest. Dermatol. http://dx.doi.org/10.1038/jid.2013.413.
11. **Harrison WJ, Bull JJ, Seltmann H, Zouboulis CC, Philpott MP.** 2007. Expression of lipogenic factors galectin-12, resistin, SREBP-1, and SCD in human sebaceous glands and cultured sebocytes. J. Invest. Dermatol. **127:**1309–1317. http://dx.doi.org/10.1038/sj.jid.5700743.
12. **Georgel P, Crozat K, Lauth X, Makrantonaki E, Seltmann H, Sovath S, Hoebe K, Du X, Rutschmann S, Jiang Z, Bigby T, Nizet V, Zouboulis CC, Beutler B.** 2005. A Toll-like receptor 2-responsive lipid effector pathway protects mammals against skin infections with gram-positive bacteria. Infect. Immun. **73:**4512–4521. http://dx.doi.org/10.1128/IAI.73.8.4512-4521.2005.
13. **Zouboulis CC, Angres S, Seltmann H.** 2011. Regulation of stearoyl-coenzyme A desaturase and fatty acid delta-6 desaturase-2 expression by linoleic acid and arachidonic acid in human sebocytes leads to enhancement of proinflammatory activity but does not affect lipogenesis. Br. J. Dermatol. **165:**269–276. http://dx.doi.org/10.1111/j.1365-2133.2011.10340.x.
14. **Sampath H, Flowers MT, Liu X, Paton CM, Sullivan R, Chu K, Zhao M, Ntambi JM.** 2009. Skin-specific deletion of stearoyl-CoA desaturase-1 alters skin lipid composition and protects mice from high fat diet-induced obesity. J. Biol. Chem. **284:**19961–19973. http://dx.doi.org/10.1074/jbc.M109.014225.
15. **Westerberg R.** 2004. Role for ELOVL3 and fatty acid chain length in development of hair and skin function. J. Biol. Chem. **279:**5621–5629. http://dx.doi.org/10.1074/jbc.M310529200.
16. **Chen HC, Smith SJ, Tow B, Elias PM, Farese RV.** 2002. Leptin modulates the effects of acyl CoA:diacylglycerol acyltransferase deficiency on murine fur and sebaceous glands. J. Clinical Invest. **109:**175–181. http://dx.doi.org/10.1172/JCI13880.
17. **Sugawara T, Nemoto K, Adachi Y, Yamano N, Tokuda N, Muto M, Okuyama R, Sakai S, Owada Y.** 2012. Reduced size of sebaceous gland and altered sebum lipid composition in mice lacking fatty acid binding protein 5 gene. Exp. Dermatol. **21:**543–546. http://dx.doi.org/10.1111/j.1600-0625.2012.01514.x.
18. **Greene RS, Downing DT, Pochi PE, Strauss JS.** 1970. Anatomical variation in the amount and composition of human skin surface lipid. J. Invest. Dermatol. **54:**240–247. http://dx.doi.org/10.1111/1523-1747.ep12280318.
19. **Zouboulis CC.** 2004. Acne and sebaceous gland function. Clin. Dermatol. **22:**360–366. http://dx.doi.org/10.1016/j.clindermatol.2004.03.004.
20. **Zouboulis CC, Boschnakow A.** 2001. Chronological ageing and photoageing of the human sebaceous gland. Clin. Exp. Dermatol. **26:**600–607. http://dx.doi.org/10.1046/j.1365-2230.2001.00894.x.
21. **Bron AJ, Tiffany JM.** 2004. The contribution of meibomian disease to dry eye. Ocul. Surf. **2:**149–164. http://dx.doi.org/10.1016/S1542-0124(12)70150-7.
22. **Wang W, Lv N, Zhang S, Shui G, Qian H, Zhang J, Chen Y, Ye J, Xie Y, Shen Y, Wenk MR, Li P.** 2012. Cidea is an essential transcriptional coactivator regulating mammary gland secretion of milk lipids. Nat. Med. **18:**235–243. http://dx.doi.org/10.1038/nm.2614.
23. **Ye J, Li JZ, Liu Y, Li X, Yang T, Ma X, Li Q, Yao Z, Li P.** 2009. Cideb, an ER- and lipid droplet-associated protein, mediates VLDL lipidation and maturation by interacting with apolipoprotein B. Cell Metab. **9:**177–190. http://dx.doi.org/10.1016/j.cmet.2008.12.013.
24. **Gong J, Sun Z, Wu L, Xu W, Schieber N, Xu D, Shui G, Yang H, Parton RG, Li P.** 2011. Fsp27 promotes lipid droplet growth by lipid exchange and transfer at lipid droplet contact sites. J. Cell Biol. **195:**953–963. http://dx.doi.org/10.1083/jcb.201104142.
25. **Zhou Z, Yon Toh S, Chen Z, Guo K, Peng Ng C, Ponniah S, Lin S-C, Hong W, Li P.** 2003. Cidea-deficient mice have lean phenotype and are resistant to obesity. Nat. Genet. **35:**49–56. http://dx.doi.org/10.1038/ng1225.
26. **Qi J, Gong J, Zhao T, Zhao J, Lam P, Ye J, Li JZ, Wu J, Zhou H-M, Li P.** 2008. Downregulation of AMP-activated protein kinase by Cidea-mediated ubiquitination and degradation in brown adipose tissue. EMBO J. **27:**1537–1548. http://dx.doi.org/10.1038/emboj.2008.92.
27. **Toh SY, Gong J, Du G, Li JZ, Yang S, Ye J, Yao H, Zhang Y, Xue B, Li Q, Yang H, Wen Z, Li P.** 2008. Up-regulation of mitochondrial activity and acquirement of brown adipose tissue-like property in the white adipose tissue of Fsp27 deficient mice. PLoS One **3:**e2890. http://dx.doi.org/10.1371/journal.pone.0002890.
28. **Maier H, Meixner M, Hartmann D, Sandhoff R, Wang-Eckhardt L, Zoller I, Gieselmann V, Eckhardt M.** 2011. Normal fur development and sebum production depends on fatty acid 2-hydroxylase expression in sebaceous glands. J. Biol. Chem. **286:**25922–25934. http://dx.doi.org/10.1074/jbc.M111.231977.
29. **Sun Z, Gong J, Wu L, Li P.** 2013. Imaging lipid droplet fusion and growth. Methods Cell Biol. **116:**253–268. http://dx.doi.org/10.1016/B978-0-12-408051-5.00013-9.
30. **Paus R, van der Veen C, Eichmuller S, Kopp T, Hagen E, Muller-Rover S, Hofmann U.** 1998. Generation and cyclic remodeling of the hair follicle immune system in mice. J. Invest. Dermatol. **111:**7–18. http://dx.doi.org/10.1046/j.1523-1747.1998.00243.x.
31. **Pappas A, Johnsen S, Liu J-C, Eisinger M.** 2009. Sebum analysis of individuals with and without acne. Dermatoendocrinol. **1:**157–161. http://dx.doi.org/10.4161/derm.1.3.8473.
32. **Shui G, Lam SM, Stebbins J, Kusunoki J, Duan X, Li B, Cheong WF, Soon D, Kelly RP, Wenk MR.** 2013. Polar lipid derangements in type 2 diabetes mellitus: potential pathological relevance of fatty acyl heterogeneity in sphingolipids. Metabolomics **9:**786–799. http://dx.doi.org/10.1007/s11306-013-0494-0.
33. **Lam SM, Tong L, Reux B, Lear MJ, Wenk MR, Shui G.** 2013. Rapid and sensitive profiling of tear wax ester species using high performance liquid chromatography coupled with tandem mass spectrometry. J. Chromatogr. A **1308:**166–171. http://dx.doi.org/10.1016/j.chroma.2013.08.016.
34. **Shui G, Guan XL, Low CP, Chua GH, Goh JSY, Yang H, Wenk MR.** 2010. Toward one step analysis of cellular lipidomes using liquid chromatography coupled with mass spectrometry: application to Saccharomyces cerevisiae and Schizosaccharomyces pombe lipidomics. Mol. Biosyst. **6:**1008–1017. http://dx.doi.org/10.1039/b913353d.
35. **Lam SM, Tong L, Duan X, Petznick A, Wenk MR, Shui G.** 2014. Extensive characterization of human tear fluid collected using different techniques unravels the presence of novel lipid amphiphiles. J. Lipid Res. **55:**289–298. http://dx.doi.org/10.1194/jlr.M044826.
36. **Shui G, Cheong WF, Jappar IA, Hoi A, Xue Y, Fernandis AZ, Tan BK-H, Wenk MR.** 2011. Derivatization-independent cholesterol analysis

in crude lipid extracts by liquid chromatography/mass spectrometry: applications to a rabbit model for atherosclerosis. J. Chromatogr. A **1218:** 4357–4365. http://dx.doi.org/10.1016/j.chroma.2011.05.011.
37. **Zouboulis CC, Seltmann H, Neitzel H, Orfanos CE.** 1999. Establishment and characterization of an immortalized human sebaceous gland cell line (SZ95). J. Invest. Dermatol. **113:**1011–1020. http://dx.doi.org/10.1046/j.1523-1747.1999.00771.x.
38. **Panteleyev AA, Paus R, Wanner R, Nurnberg W, Eichmuller S, Thiel R, Zhang J, Henz BM, Rosenbach T.** 1997. Keratin 17 gene expression during the murine hair cycle. J. Invest. Dermatol. **108:**324–329. http://dx.doi.org/10.1111/1523-1747.ep12286476.
39. **Chen W, Kelly MA, Opitz-Araya X, Thomas RE, Low MJ, Cone RD.** 1997. Exocrine gland dysfunction in MC5-R-deficient mice: evidence for coordinated regulation of exocrine gland function by melanocortin peptides. Cell **91:**789–798. http://dx.doi.org/10.1016/S0092-8674(00)80467-5.
40. **Driver PJ, Lemp MA.** 1996. Meibomian gland dysfunction. Surv. Ophthalmol. **40:**343–367. http://dx.doi.org/10.1016/S0039-6257(96)80064-6.
41. **Foulks GN, Bron AJ.** 2003. Meibomian gland dysfunction: a clinical scheme for description, diagnosis, classification, and grading. Ocul. Surf. **1:**107–126. http://dx.doi.org/10.1016/S1542-0124(12)70139-8.
42. **Nicolaides N, Fu HC, Rice GR.** 1968. The skin surface lipids of man compared with those of eighteen species of animals. J. Invest. Dermatol. **51:**83–89.
43. **Mayer JA, Foley J, De La Cruz D, Chuong C-M, Widelitz R.** 2008. Conversion of the nipple to hair-bearing epithelia by lowering bone morphogenetic protein pathway activity at the dermal-epidermal interface. Am. J. Pathol. **173:**1339–1348. http://dx.doi.org/10.2353/ajpath.2008.070920.
44. **Viswakarma N, Yu S, Naik S, Kashireddy P, Matsumoto K, Sarkar J, Surapureddi S, Jia Y, Rao MS, Reddy JK.** 2007. Transcriptional regulation of Cidea, mitochondrial cell death-inducing DNA fragmentation factor-like effector A, in mouse liver by peroxisome proliferator-activated receptor alpha and gamma. J. Biol. Chem. **282:**18613–18624. http://dx.doi.org/10.1074/jbc.M701983200.
45. **Hallberg M, Morganstein DL, Kiskinis E, Shah K, Kralli A, Dilworth SM, White R, Parker MG, Christian M.** 2008. A functional interaction between RIP140 and PGC-1 regulates the expression of the lipid droplet protein CIDEA. Mol. Cell. Biol. **28:**6785–6795. http://dx.doi.org/10.1128/MCB.00504-08.
46. **Akamatsu H, Zouboulis CC, Orfanos CE.** 1992. Control of human sebocyte proliferation in vitro by testosterone and 5-alpha-dihydrotestosterone is dependent on the localization of the sebaceous glands. J. Invest. Dermatol. **99:**509–511. http://dx.doi.org/10.1111/1523-1747.ep12616181.